Study of diphoton decays of the lightest scalar Higgs boson in the Next-to-Minimal Supersymmetric Standard Model[*]

FAN Jia-Wei(范嘉伟)[1,2,3]   TAO Jun-Quan(陶军全)[1;1)]   SHEN Yu-Qiao(沈玉乔)[1,2]   CHEN Guo-Ming(陈国明)[1]

CHEN He-Sheng(陈和生)[1]   S. Gascon-Shotkin[3]   M. Lethuillier[3]   L. Sgandurra[3]   P. Soulet[3]

[1] Institute of High Energy Physics, Chinese Academy of Sciences, Beijing 100049, China
[2] University of Chinese Academy of Sciences, Beijing 100049, China
[3] Institut de Physique Nucléaire de Lyon, Université de Lyon, Université Claude Bernard Lyon 1, CNRS-IN2P3, Villeurbanne 69622, France

Abstract: The CMS and ATLAS experiments at the LHC have announced the discovery of a Higgs boson with mass at approximately 125 GeV/c^2 in the search for the Standard Model Higgs boson via, notably, the $\gamma\gamma$ and ZZ to four leptons final states. Considering the recent results of the Higgs boson searches from the LHC, we study the lightest scalar Higgs boson h_1 in the Next-to-Minimal Supersymmetric Standard Model by restricting the next-to-lightest scalar Higgs boson h_2 to be the observed to the 125 GeV/c^2 state. We perform a scan over the relevant NMSSM parameter space that is favoured by low fine-tuning considerations. Moreover, we also take the experimental constraints from direct searches, B-physics observables, relic density, and anomalous magnetic moment of the muon measurements, as well as the theoretical considerations, into account in our specific scan. We find that the signal rate in the two-photon final state for the NMSSM Higgs boson h_1 with the mass range from about 80 GeV/c^2 to about 122 GeV/c^2 can be enhanced by a factor of up to 3.5 when the Higgs boson h_2 is required to be compatible with the excess from latest LHC results. This motivates the extension of the search at the LHC for the Higgs boson h_1 in the diphoton final state down to masses of 80 GeV/c^2, particularly with the upcoming proton-proton collision data to be taken at center-of-mass energies of 13–14 TeV.

Key words: Supersymmetry, Next-to-Minimal Supersymmetric Standard Model, lightest scalar Higgs boson

PACS: 11.30.Pb, 14.80.Cp   **DOI:** 10.1088/1674-1137/38/7/073101

1   Introduction

The Standard Model (SM) of particle physics has been very successful in explaining high-energy experimental results. One of the remaining questions is to find the source of mass. The solution to this question in the SM is given by the mechanism introduced by Higgs, Englert and Brout [1–3], which introduces an additional scalar field whose quantum, the so-called Higgs boson, should be experimentally observable. In July 2012, a Higgs boson-like particle with mass at approximately 125 GeV/c^2 was announced to have been discovered by the two experiments, ATLAS and CMS, independently at the LHC via, notably, the two most promising channels: H → $\gamma\gamma$ and H → ZZ* channel with a four-lepton final state [4–7]. Meanwhile, the Tevatron collaborations also announced their new Higgs boson search re-

sults, based mainly on VH associated production with H → b$\bar{\text{b}}$ decay channel [8], which supported the LHC ∼125 GeV/c^2 Higgs boson-like particle discovery results. However, the observed signal strength is somewhat biased against the SM prediction within 1 or 2 times of the experimental uncertainty in each final state, as seen from the Appendix. More data should be accumulated in order to test, with higher precision, the discrepancies between the data analysis results and the SM predictions on the signal strength. If the bias still exists with a more precise measurement in the future, then it could provide a window to new physics Beyond the Standard Model (BSM).

Supersymmetry (often abbreviated SUSY) [9–12] is one of the theoretical options for BSM physics. It introduces a new symmetry between fermions and bosons.

The most common SUSY framework is the Minimal

Supersymmetric Standard Model (MSSM) [13–15], which keeps the number of new fields and couplings to a minimum. In the MSSM, the Higgs sector contains two Higgs doublets, which leads to a spectrum including two CP-even, one CP-odd, and two charged Higgs bosons. The Lagrangian of the MSSM contains a supersymmetric mass term, the μ-term. This mass term is invariant under supersymmetry and, therefore, it seems unrelated to the electroweak scale, although it is phenomenologically required to be in this scale. This leads to the well known "μ problem" [16, 17] in the MSSM. The simplest solution to this problem is the so-called Next-to-Minimal Supersymmetric Standard Model (NMSSM) [18] that introduces a new gauge singlet superfield, which only couples to the Higgs sector in a similar way as the Yukawa coupling and can give rise to an effective μ-term to solve the "μ problem". Meanwhile, this new singlet adds additional degrees of freedom to the NMSSM particle spectrum. In the CP conserving case, which is assumed in this paper, the states in the Higgs sector can be classified as three CP-even Higgs bosons h_i (i=1, 2, 3), two CP-odd Higgs bosons a_j (j=1, 2), and two charged Higgs bosons $h^\pm$, for a total of seven observable states.

The extended parameter space of the NMSSM gives rise to a rich and interesting phenomenology, which is particularly related to the two lightest CP-even Higgs bosons h_i (i=1, 2). Inspired by the discovery of the new particle with mass at approximately 125 GeV/c^2 from the LHC, and also the small LEP excess (approximately 2σ) at about 98 GeV/c^2 in $e^+e^- \to$ Zh with $h \to b\bar{b}$ [19, 20], in this paper we study the lightest CP-even Higgs bosons h_1 in a mass range down to approximately 80 GeV/c^2 by assuming the next-to-lightest CP-even Higgs boson h_2 as the new particle at m $\sim$125 GeV/c^2. The third CP-even Higgs boson is out of reach of current experiments due to its low cross section in our scanned parameter ranges. To distinguish our study from many other NMSSM studies [21–25], we mainly focus on the regions of parameter space favoured by low fine-tuning [23] considerations, with an sbottom mass of order 400 GeV/c^2 to 1 TeV/c^2, which is compatible with the SUSY search results at the LHC [26–28], the effective μ parameter between 100–200 GeV/c^2, and also low tanβ within a range from 3 to 4. Furthermore, we perform our scan over the parameter space, which can explain both dark matter [29], (g−2) [30] and some other experimental constraints, which are described in Section 3. To completely test the compatibility of our chosen region of parameter space with the recent LHC results, we interface the package NMSSMTools (version 4.1.0) [31] with the newly public packages HiggsBounds-4 [32] and

HiggsSignal-1 [33][1].   Additionally, we show in section 4 that the $h_2 \to$ XX (XX represents $\gamma\gamma$, ZZ, WW, $\tau\tau$, or bb) signal strengths can be compatible with the current experimental results, that signal strengths for an h1 with a mass below 110 GeV/c^2 having higher values than currently predicted by the SM are possible, and that the current sensitivities of the LHC experiments are such that such a Higgs boson h1 could be detected.

The structure of this paper is organized as follows. In Section 2, we briefly introduce the Higgs sector of the NMSSM. The details of the parameter ranges we chose for the scan in the NMSSM parameter space are described in Section 3. Section 4 shows the results of our numerical study, including the Higgs boson h_2 signal strength in each decay mode and the discussion on the lightest scalar Higgs boson h_1. The summary and outlook are given in Section 5.

2   The NMSSM and Higgs boson signal strengths

2.1   Brief description of the NMSSM

The general NMSSM includes two Higgs superfields $\hat{H}_u$, $\hat{H}_d$ and one additional gauge singlet chiral superfield $\hat{S}$. To start, we consider the NMSSM with a scale invariant superpotential W_{NMSSM}, and the corresponding soft SUSY-breaking masses and couplings L_{soft}, both of which are limited to the R-parity and CP-conserving case. The superpotential W_{NMSSM} depending on the Higgs superfields $\hat{H}_u$, $\hat{H}_d$ and $\hat{S}$ is [18]

$$W_{NMSSM} = h_u \hat{Q}\cdot\hat{H}_u\hat{U}_R^c + h_d \hat{H}_d\cdot\hat{Q}\hat{D}_R^c + h_e \hat{H}_d\cdot\hat{L}\hat{E}_R^c + \lambda \hat{S}\hat{H}_u\cdot\hat{H}_d + \frac{1}{3}\kappa\hat{S}^3. \tag{1}$$

On the right-hand side of the above formula, the first three terms are the Yukawa couplings of the quark and lepton superfields. The fourth term replaces the μ-term $\mu\hat{H}_u\hat{H}_d$ of the MSSM superpotential. The last term, which is the cubic in the singlet superfield, is introduced to avoid the appearance of a Peccei-Quinn axion, which is tightly constrained by cosmological observation [18]. The corresponding soft SUSY-breaking masses and couplings are given in the SLHA2 [35] conventions by [18]

$$-L_{soft} = m_{H_u}^2|H_u|^2 + m_{H_d}^2|H_d|^2 + m_S^2|S|^2 + m_Q^2|Q|^2$$
$$+ m_U^2|U_R|^2 + m_D^2|D_R|^2 + m_L^2|L|^2 + m_E^2|E_R|^2$$
$$+ h_u A_u Q\cdot H_u U_R^c - h_d A_d Q\cdot H_d D_R^c - h_e A_e L\cdot H_d E_R^c$$
$$+ \lambda A_\lambda H_u\cdot H_d S + \frac{1}{3}\kappa A_\kappa S^3 + \text{h.c.}. \tag{2}$$

---

1) The LHC H125 constraints have been implemented in the current version of NMSSMTools [34]. But this version was not available at the start of this work. We have recently checked that the implementation of the H125 constraints in NMSSMTools and HiggsSignals gives similar results, even though they are not strictly identical.

In Eq. (1) and Eq. (2), clearly the non-zero vacuum expectation value s of the singlet $\hat{S}$ of the order of the weak or SUSY-breaking scale gives rise to an effective μ-term with

$$\mu_{\text{eff}} = \lambda s, \tag{3}$$

which solves the "μ problem" of the MSSM. Meanwhile, the three SUSY-breaking mass-squared terms for H_{u}, H_{d} and S appearing in L_{soft} can be expressed in terms of their VEVs (Vacuum Expectation Value) through the three minimization conditions of the scalar potential. Therefore, the Higgs sector of the NMSSM is described by the following six parameters

$$\lambda, \kappa, A_{\lambda}, A_{\kappa}, \tan\beta = \frac{\langle H_{\text{u}} \rangle}{\langle H_{\text{d}} \rangle}, \ \mu_{\text{eff}} = \lambda \langle S \rangle, \tag{4}$$

in which each pair of brackets denote the VEV of the respective field inside them. In addition to these six parameters of the Higgs sector, during the scan (as described below) we need to specify the squark and slepton soft SUSY-breaking masses and the trilinear couplings, as well as the gaugino soft SUSY-breaking masses, to describe the model completely.

2.2   Signal strength of Higgs boson

As in the SM, the main Higgs boson production processes include gluon-gluon fusion, vector boson fusion, Higgs-strahlung and associated production with a vector boson or $t\bar{t}$. The most dominant process is gluon-gluon fusion, followed by vector boson fusion, while the other two only play a minor role in the SM. In this paper, we will take all four production processes into account.

We are interested in the Higgs boson signal strengths $\mu_{\text{XX}}^{\text{h}_i}$ (XX=$\gamma\gamma$, ZZ, WW, bb, $\tau\tau$), which are the relative ratios of the cross section times branching ratio $(R_{\text{XX}}^{\text{h}_i} = \sigma(\text{pp} \rightarrow \text{h}_i) \times BR(\text{h}_i \rightarrow \text{XX}))$ to the SM predicted value: $\mu_{\text{XX}}^{\text{h}_i} = R_{\text{XX}}^{\text{h}_i}/(R_{\text{XX}}^{\text{h}_i})_{\text{SM}}$.

In the NMSSM framework, the couplings of the Higgs bosons h_1 and h_2 depend on their decompositions into the CP-even weak eigenstates H_{d}, H_{u} and S, which are given by [18]

$$\begin{aligned} h_1 &= a_{1,\text{d}} H_{\text{d}} + a_{1,\text{u}} H_{\text{u}} + a_{1,\text{s}} S, \\ h_2 &= a_{2,\text{d}} H_{\text{d}} + a_{2,\text{u}} H_{\text{u}} + a_{2,\text{s}} S. \end{aligned} \tag{5}$$

Then, the reduced tree-level couplings of h_i ($i=1,2$) to b quarks, t quarks, and electroweak gauge bosons V relative to the SM value are

$$\frac{g_{\text{h}_i\text{bb}}}{g_{\text{h}_{\text{SM}}\text{bb}}} = \frac{a_{i,\text{d}}}{\cos\beta}, \quad \frac{g_{\text{h}_i\text{tt}}}{g_{\text{h}_{\text{SM}}\text{tt}}} = \frac{a_{i,\text{u}}}{\sin\beta},$$
$$\frac{g_{\text{h}_i\text{VV}}}{g_{\text{h}_{\text{SM}}\text{VV}}} = \cos\beta a_{i,\text{d}} + \sin\beta a_{i,\text{u}}. \tag{6}$$

For the low values of $\tan\beta$ considered in this paper, the couplings of the Higgs bosons to photons are induced by loop diagrams, which are dominated by top-quark

loops. As stated above, deduced from the the coupling of Higgs boson to top-quark, also considering the contributions from non-SM particles in the loops (mainly the stop squark) [36], the Higgs boson branching ratio into two photons can be enhanced in some specific portions of parameter space.

3   Scans with constrained parameters

In the following, we will perform a specific scan in the NMSSM parameter space, which favours the Higgs boson h_2 corresponding to the state with mass value in the neighborhood of 125 GeV/c^2, and is compatible with the recent LHC results and the Higgs boson h_1 having mass restricted in the range down to $\sim$80 GeV/c^2. The program package NMSSMTools (version 4.1.0) [31] is used to compute the SUSY particle and NMSSM Higgs boson spectrum and branching ratios. NMSSMTools contains four subpackages: NMHDECAY, NMSDECAY, NMSPEC and NMGMSB. The Fortran code NMHDECAY provides the Higgs boson masses, decay widths and branching ratios that will be used in this paper. Furthermore, the NMSSMTools package applies the constraints from theory, low-energy observables in Tevatron and LEP, some bounds from direct searches of SUSY particles in LHC [26–28], relic density Ωh^2 [29], B-physics observables such as $BR(\text{B} \rightarrow \text{X}_{\text{s}}\gamma)$, $BR(\text{B}_{\text{s}} \rightarrow \mu^+\mu^-)$, $BR(\text{B}_{\mu} \rightarrow \tau^+\nu_{\tau})$ and the mass mixings ΔM_{s}, ΔM_{d} [37–40], and the anomalous magnetic moment of the muon $(g-2)$ constraints [30]. All these constraints are used to perform our scan. More details on the implementation of all these constraints in the package can be checked from the webpage of the NMSSMTools program [31].

After careful study, we are guided to use the following parameter ranges by theoretical and experimental considerations:

1) To keep the large doublet-singlet mixing in the Higgs sector, we are more interested in large values of λ, κ (but small enough to avoid Landau pole below GUT scale) and low values of $\tan\beta$, which naturally keep the amount of fine-tuning as low as possible. Considering the anomalous magnetic moment of the muon $(g-2)$ constraint, we keep μ_{eff} positive with minimal variations in order to avoid fine-tuning. Hence, the four parameters are constrained in the following ranges [30]

$$\begin{aligned} 0.6 < \lambda < 0.75, \quad 0.2 < \kappa < 0.3, \quad 3 < \tan\beta < 4, \\ 165 \text{ GeV}/c^2 < \mu_{\text{eff}} < 190 \text{ GeV}/c^2. \end{aligned} \tag{7}$$

2) The soft SUSY-breaking trilinear couplings A_{λ} and A_{κ} are varied in the ranges [18]

$$\begin{aligned} -100 \text{ GeV}/c^2 < A_{\kappa} < -50 \text{ GeV}/c^2, \\ 610 \text{ GeV}/c^2 < A_{\lambda} < 630 \text{ GeV}/c^2. \end{aligned} \tag{8}$$

We remark that, constraining the parameters A_λ and A_κ in these ranges favor h_1 with higher signal strength as well as being in the mass range down to ~ 80 GeV/c^2.

3) In order to compare with the recent LHC search bounds [26–28], we conservatively set the left-handed soft SUSY-breaking masses of the squark sector ($M_{\tilde{Q}_{1,2}}$) and right-handed soft SUSY-breaking sup masses ($M_{\tilde{u}_R}$ and $M_{\tilde{c}_R}$) to 2500 GeV/c^2, both of which are in the first two generations. We take low values of soft SUSY-breaking masses of the slepton sector ($M_{\tilde{L}_{1,2,3}}$, $M_{\tilde{e}_R}$, $M_{\tilde{\mu}_R}$ and $M_{\tilde{\tau}_R}$) as 300 GeV/c^2 to follow the $(g-2)$ constraint [30]. Furthermore, we set the right-handed soft SUSY-breaking masses ($M_{\tilde{D}_R}$) and the trilinear couplings (A_D, A_E and A_U) to 2500 GeV/c^2 and 1000 GeV/c^2, respectively. This results in a light sbottom mass of approximately 400 GeV/$c^2 < M_{\tilde{b}_1} < 1000$ GeV/c^2, which is compatible with the recent LHC SUSY results. Hence, we have

$$M_{\tilde{u}_R} = M_{\tilde{c}_R} = M_{\tilde{Q}_{1,2}} = 2500 \text{ GeV}/c^2,$$
$$M_{\tilde{L}_{1,2}} = M_{\tilde{e}_R} = M_{\tilde{\mu}_R} = 300 \text{ GeV}/c^2,$$
$$M_{\tilde{L}_3} = M_{\tilde{\tau}_R} = 300 \text{ GeV}/c^2,$$
$$M_{\tilde{D}_R} = 2500 \text{ GeV}/c^2 \quad (\text{D}=\text{d,s,b}), \qquad (9)$$
$$A_D = A_E = 1000 \text{ GeV}/c^2,$$
$$A_U = 1000 \text{ GeV}/c^2.$$

4) The Higgs sector is strongly influenced by the stop sector via radiative corrections [41]. In addition, for fine-tuning reasons, we further need to specify the soft SUSY-breaking masses of the stop sector. We modify the NMSSMTools code in order to constrain them to be rather low. After studying the properties of these parameters, we vary them simultaneously within

$$550 \text{ GeV}/c^2 < M_{\tilde{Q}_3} = M_{\tilde{t}_R} < 700 \text{ GeV}/c^2. \qquad (10)$$

(Eqs. (9) and (10) presuppose a SUSY scale.)

5) Concerning the relic density constraint [29], the remaining gaugino soft SUSY-breaking masses are set to be within

$$100 \text{ GeV}/c^2 < M_1 < 150 \text{ GeV}/c^2,$$
$$180 \text{ GeV}/c^2 < M_2 < 300 \text{ GeV}/c^2, \qquad (11)$$
$$M_3 = 1000 \text{ GeV}/c^2.$$

Then, we perform our scan after the application of the constraints on the parameters as described above.

4   Numerical study

In Section 2, we introduced the production processes and the signal strengths of the NMSSM Higgs bosons. In this section, we demonstrate that the constraints on the parameters as described in the above section can produce

a next-to-lightest NMSSM scalar Higgs boson h_2 that is compatible with the observed state at the LHC with mass at approximately 125 GeV/c^2. We concentrate our study on the lightest NMSSM scalar Higgs boson h_1. Considering the relic density Ωh^2, we will focus on two cases, $\Omega h^2 < 0.1102$ (named case I) and $0.1102 < \Omega h^2 < 0.1272$ (the "WMAP" window [42], named case II). In all plots below, points for case I are represented by blue squares and case II by red triangles.

4.1   Mass distributions of the NMSSM Higgs bosons

Based on the constrained parameters, we firstly show the mass distributions of the two lightest NMSSM scalar Higgs bosons h_1 and h_2 in Fig. 1. As can be seen, most of the parameter points cluster around mass values centered around 125 GeV/c^2 for M_{h_2} in case I and case II. We conclude that the parameter ranges are correctly chosen to give a mass of the Higgs boson h_2 close to 125 GeV/c^2. Considering the lightest NMSSM scalar Higgs boson h_1, it is clear that its mass can lie in a wide range, from approximately around 80 GeV/c^2 to 122 GeV/c^2 for both cases. We point out that the excluded region below 114.7 GeV/c^2 at LEP [19] could still be allowed in the context of the NMSSM for points in the parameter phase space where the production rate of h_1 into bb and $\tau\tau$ (the channels searched for at LEP) are reduced or suppressed with respect to the SM.
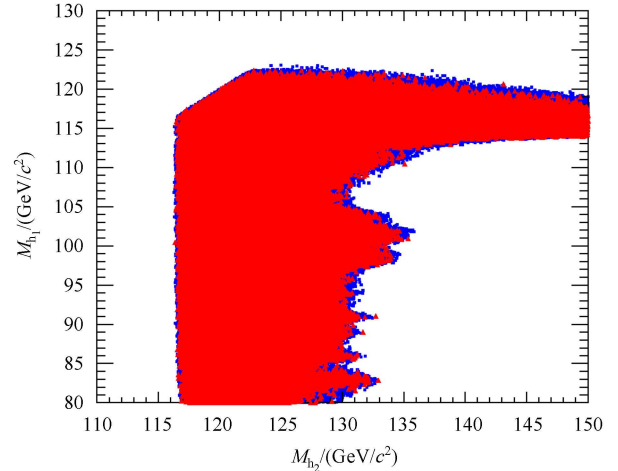

Fig. 1.   (color online) The NMSSM Higgs boson mass spectrum in M_{h_1} vs. M_{h_2}. Points for case I are represented by blue squares and case II by red triangles.

4.2   Signal strengths of the NMSSM Higgs boson h_2

In the NMSSM framework, not all of the $\mu_{XX}^{h_i}$ ($i=1, 2$) are independent, for example, $\mu_{ZZ}^{h_i} = \mu_{WW}^{h_i}$. Only the reduced couplings are calculated by NMSSMTools, we use

the absolute values in the SM [43] to calculate the total signal strength, including the four production modes mentioned in Section 2.2. We also check that the differences of weights of the production mode are quite negligible between 7 and 8 TeV with respect to experimental uncertainties. Two new public tools are utilized in order to further test whether a given point in our scanned parameter space is allowed or excluded by the recent LEP, Tevatron, and LHC results at 95% confidence level (CL).

We use the public tool HiggsBounds-4 [32] to further compare Higgs sector predictions with existing exclusion limits of various search channels. The SLHA format files calculated by NMSSMTools are used as the inputs for HiggsBounds-4. The main algorithm of HiggsBounds can be described in two steps. In the first step the Higgs-Bounds uses the expected experimental limits from LEP, Tevatron, and the LHC [8, 19, 44, 45] to determine which decay channel has the highest statistical sensitivity. In the second step, only for this particular channel, the theory prediction is compared to the observed experimental limits in order to conclude whether this parameter point is allowed or excluded at 95% CL.

Compatibility with the measured mass and rates of the observed new state having a mass of $\sim$125 GeV/c^2 is then imposed, using the public code HiggsSignal-1 [33]. The HiggsSignal-1 takes the predictions of an arbitrary model (here the NMSSM) as an input, providing a quantitative answer to the statistical question of how compatible the model predictions are with the Higgs boson search experimental results, especially signal strengths and the measured mass, by evaluating a χ^2 calculation. The main results from HiggsSignal-1, which are used to further constrain our parameter space, are reported in the form of a χ^2 value and an associated p-value. We consider that the given parameter point is compatible with the experimental constraints only if the p-value given by HiggsSignal-1 is greater than 0.05. By using these two programs in parallel, we obtain the most complete test for the scanned NMSSM parameter space.

The allowed values for μ_{XX}^{h2} from the scan over the NMSSM parameter space are shown in Fig. 2, where all of the constraints described in section 3 have been applied. The results are shown before and after applying the additional constraints from the above two programs. We first show $\mu_{\gamma\gamma}^{h2}$ plotted versus μ_{XX}^{h2} (XX=ZZ, WW, bb, $\tau\tau$). The points including error bars represent the latest LHC public results for the best fit values of the signal strengths μ_{XX}^{h2} with uncertainties in the different final states, as reported by the CMS and ATLAS collaborations [44, 45]. The values and errors are listed in Table A1 in the Appendix [6, 7, 44, 45]. It is clearly visible that the parameter points compatible with both HiggsBounds-4 and HiggsSignal-1 provide theoretical predictions which are consistent with the experimental results. In Fig. 2,
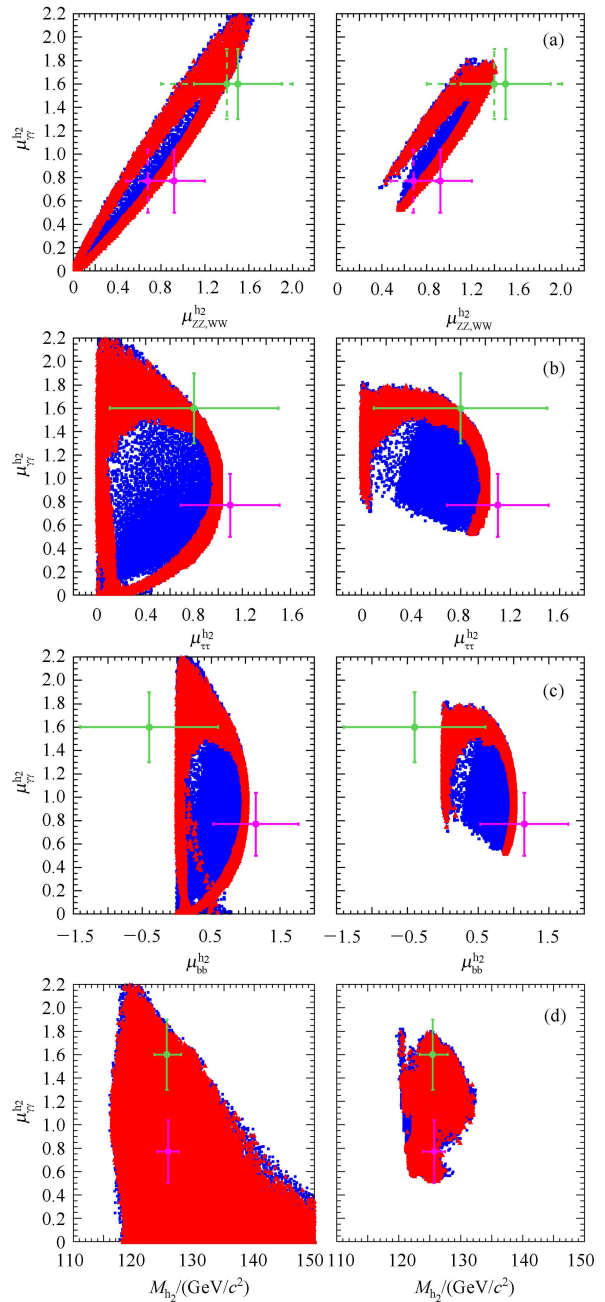

Fig. 2. The signal strength of $\gamma\gamma$ versus signal strengths of ZZ(WW) in (a), bb in (b), $\tau\tau$ in (c) and the mass of the NMSSM Higgs boson h_2 in (d). The results shown in the left-hand (right-hand) plots are obtained before (after) applying the constraints from HiggsBounds-4 and HiggsSignal-1. The magenta solid point for the mean value and line for the uncertainties represent the CMS results while those in green represent the ATLAS results. Points for case I are represented by blue squares and case II by red triangles. In (a), the solid point and line represent the results from ZZ final state while the dashed line corresponds to WW final state.

by taking the di-photon final state as an example, we also show the signal strength $\mu_{\gamma\gamma}^{h_2}$ plotted against its mass in Fig. 2(d). From the right-hand plot, the $\mu_{\gamma\gamma}^{h_2}$ values cover the range 0.5 to 1.8 while the mass is in the range 120 GeV/c^2 to 132 GeV/c^2, both of which are consistent with the new observed state within errors. It is clearly visible that the NMSSM can produce rates that are compatible with both the CMS and ATLAS results for both relic density cases. The plots show that the relatively sizable enhancements with respect to the SM rates for the $\gamma\gamma$ and ZZ final states reported by ATLAS are possible in the vicinity of 125 GeV/c^2 in the NMSSM framework and are also possible for the relatively suppressed rates reported by CMS.

4.3   Branching ratio and signal strength of the NMSSM Higgs boson h_1

We will now focus our discussion on the lightest NMSSM scalar Higgs boson h_1 by looking at the diphoton final state, and will further restrict ourselves to the case of CMS results only.

Apart from the constraints mentioned in previous sections, we now demand in addition that the NMSSM Higgs boson h_2 fulfill mass and signal strength conditions. Considering the recent CMS results [7], the SM-like Higgs boson mass has been measured to be 125.7$\pm$0.3(stat.)$\pm$0.3(syst.) GeV/c^2. Assuming 3σ error, where σ is taken as the linear sum of the above statistical and systematic uncertainties, the mass of h_2 is constrained within the range

$$123.9 \text{ GeV}/c^2 < M_{h_2} < 127.5 \text{ GeV}/c^2. \qquad (12)$$

We also demand that the signal strength $\mu_{\gamma\gamma}^{h_2}$ should be within 1σ (taking as σ the uncertainty shown in Appendix A) of the CMS measured value:

$$0.5 \lesssim \mu_{\gamma\gamma}^{h_2} \lesssim 1.04. \qquad (13)$$

Based on these additional constraints, Fig. 3 shows the allowed values for the branching ratio of the $h_1 \to \gamma\gamma$ decay mode in the NMSSM. The cyan solid line shows the quantity including error bands evaluated in the SM for the same mass [43]. From the plots it can be seen that most of the points show that an enhanced branching ratio relative to that in the SM is possible for both relic density cases. The theoretical explanation for this enhanced two-photons branching ratio has already been introduced in Section 2.2.

In Fig. 4, we display the possible signal strengths $\mu_{\gamma\gamma}^{h_1}$ plotted against the Higgs boson h_1 mass. As seen from Fig. 4, the remaining points selected after application of all of the conditions discussed in Sections 3 and 4.2 indicate the possibility of the h_1 mass lying in the range between 80 GeV/c^2 to 122 GeV/c^2 for both relic density cases. Turning to the signal strength $\mu_{\gamma\gamma}^{h_1}$, the

figure shows that a sizable enhancement over the SM rate is possible for the Higgs boson h_1 for both relic density cases, reaching values as high as 3.5, corresponding to an h_1 mass of ~ 90 GeV/c^2. We note that, for the mass range between 100 GeV/c^2 and 110 GeV/c^2, the allowed signal strengths $\mu_{\gamma\gamma}^{h_1}$ are rather low, falling to $\sim$0.9. Nevertheless, it would still be possible to detect this low-
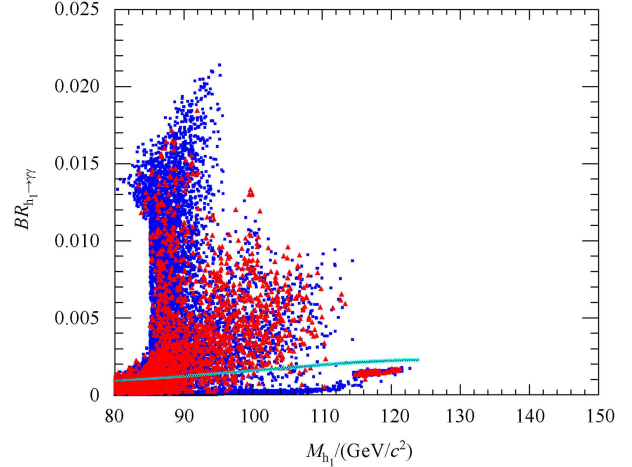

Fig. 3.   Results from the NMSSM parameter scan for the branching ratio of $h_1 \to \gamma\gamma$. The cyan solid line represents the corresponding SM value for the same mass. Points for case I are represented by blue squares and case II by red triangles.
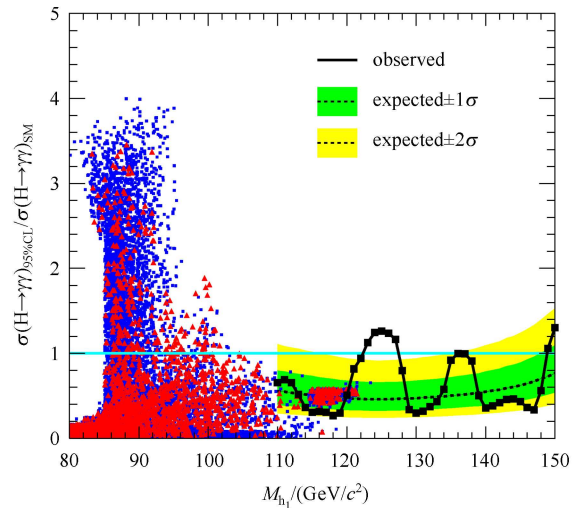

Fig. 4.   Expected and observed exclusion limits on the signal strength from CMS [44] compared with the possible signal strengths of the process pp $\to$ $h_1 \to \gamma\gamma$ from the NMSSM parameter scan. Points for case I are represented by blue squares and case II by red triangles. The solid black line together with the black squares corresponds to the ratio of the CMS observed cross sections with respect to the SM predictions, and the dashed line is the expected ratio.

mass NMSSM Higgs boson in this channel, especially with the higher energy and higher integrated luminosity in the future 13 and 14-TeV proton-proton collisions at the LHC.

In order to compare with our signal strength $\mu_{\gamma\gamma}^{h_1}$, we also superpose the official CMS public exclusion limit plot in Fig. 4. The yellow and green regions correspond to the uncertainties at 95% and 68% confidence interval, respectively, and the cyan solid line corresponds to the SM value. It is clearly seen that the NMSSM points above the solid black line (representing the CMS observed exclusion limit) are almost excluded by the CMS result in the mass range 110 GeV/c^2 to 122 GeV/c^2. We note that there is a small interesting region that is favoured by a cluster of parameter points in the neighborhood of 120 GeV/c^2. In particular, the points below 120 GeV/c^2 are already excluded by comparing with the solid black line. The remaining points lying between 120 and 122 GeV/c^2 could constitute a case of a so-called "degenerate Higgs boson" [46]. Although this is outside the scope of our discussion in this paper, it would be advisable to test this interesting scenario with the increased quantity of data and improved resolution in the future 13 and 14-TeV collisions at the LHC. To date, the present experimental results from the LHC do not cover the lower Higgs boson mass range between 80–110 GeV/c^2 in the H→γγ decay channel. In order to be able to make a conclusion for the NMSSM points in this mass range, which show the potential for sizeably enhanced signal strengths in the diphoton decay channel with respect to those predicted in the SM, a detailed analysis is needed that particularly takes account of the Z→ee background faking the diphoton signals. If the limit curve were to be extrapolated down to a mass of ~ 80 GeV/c^2, and the measurement of the signal strength is improved in the future experimental analysis, most of the NMSSM

parameter space shown in Fig. 4 could be probed.

5   Summary and outlook

In this paper, we have performed a scan in the NMSSM, focusing on the regions of parameter space favoured by low fine-tuning considerations. We have studied the lightest scalar Higgs boson h_1, including the mass and the relative signal strength in the SM prediction, especially for Higgs bosons decaying into the di-photon final state, by assuming that the second-lightest scalar Higgs boson h_2 corresponds to the observed ~ 125 GeV/c^2 state at the LHC. We find that a significant excess of the signal strength relative to that of the SM in pp→h_1→γγ up to a factor ~ 3.5 is possible in the NMSSM, especially for the mass range below the LEP bound of 114.7 GeV/c^2. We recommend that experiments extend the exclusion limit to this low-mass region in order to investigate the possibilities of the NMSSM in more detail.

With future LHC data, the best fit values of the signal strengths in each channel may evolve and the uncertainties improve, which may result in changes in the experimental results and reduced error bars in our plots. Additionally, the allowed regions in NMSSM parameter space for the interesting Higgs boson h_1 may also change. With the upcoming 13 and 14-TeV collisions at LHC, the signal for the low-mass NMSSM Higgs boson h_1 could still be detected by the experiments due to the higher collision energy and integrated luminosity.

Appendix A

Best fit values of the signal strength

Table A1.   Best fit values (μ) of the signal strength reported by CMS and ATLAS Collaborations [6, 7, 44, 45].

experiment	final state	($\sqrt{s}$/TeV, L/fb^{-1})	μ
CMS	γγ	(7, 5.1)+(8, 19.6)	0.77±0.27
CMS	ZZ	(7, 5.1)+(8, 19.6)	0.92±0.28
CMS	WW	(7, 4.9)+(8, 19.5)	0.68±0.20
CMS	bb	(7, 4.9)+(8, 12.1)	1.15±0.62
CMS	ττ	(7, 4.9)+(8, 19.4)	1.10±0.41
ATLAS	γγ	(7, 4.8)+(8, 20.7)	1.6±0.30
ATLAS	ZZ	(7, 4.6)+(8, 20.7)	1.5±0.40
ATLAS	WW	(8, 13)	1.4±0.60
ATLAS	bb	(7, 4.7)+(8, 13)	−0.4±1.00
ATLAS	ττ	(7, 4.6)+(8, 13)	0.8±0.70

References

1 Englert F, Brout R. Phys. Rev. Lett., 1964, **13**: 321
2 Higgs P W. Phys. Rev. Lett., 1964, **13**: 508
3 Guralnik G, Hagen C, Kibble T. Phys. Rev. Lett., 1964, **13**: 585
4 CMS collaboration. Phys. Lett. B, 2012, **716**: 30
5 ATLAS collaboration. Phys. Lett. B, 2012 **716**: 1
6 ATLAS collaboration. ATLAS-CONF-**2013-014**, https://twiki. cern.ch/twiki/bin/view/AtlasPublic/HiggsPublicResults
7 CMS collaboration. CMS-HIG-**13-005**, https://twiki.cern.ch/ twiki/bin/view/CMSPublic/PhysicsResultsHIG
8 CDF and D0 collaborations. arXiv: hep-ex/1303.6346v1
9 Fayet P. Phys. Lett. B, 1976, **64**: 159
10 Fayet P. Phys. Lett. B, 1977, **69**: 489
11 Farrar G R, Fayet P. Phys. Lett. B, 1978, **76**: 575
12 Giudice G F, Luty M A, Murayama H, Rattazzi R. J. High Energy Phys., 1998, **12**: 027
13 Nilles H P. Phys. Rept., 1984, **110**: 1-60
14 Haber H E, Kane G L. Phys. Rept., 1985, **117**: 75
15 Barbieri R. Riv. Nuovo Cim., 1988, **11**: 1
16 Giudice G F, Masiero A. Phys. Lett. B, 1998, **206**: 480
17 Kim J E, Nilles H P. Phys. Lett. B, 1984, **138**: 150
18 Ellwanger U, Hugonie C, Teixeira A M. Phys. Rept., 2010, **496**: 1-77
19 Barate R et al. Phys. Lett. B, 2003, **565**: 61
20 Bélanger G, Ellwanger U, Gunion J F et al. J. High Energy Phys., 2013, **1301**: 069
21 CAO J, HENG Z, LI D, YANG J M. Phys. Lett. B, 2012, **710**: 665
22 Gunion J F, Jiang Y, Kraml S. Phys. Lett. B, 2012, **710**: 454
23 King S F, Muhlleitner M, Nevzorov R. Nucl. Phys. B, 2012, **860**: 207
24 Badziak M, Olechowski M, Pokorski S. J. High Energy Phys., 2013, **1306**: 043
25 Barbieri R, Buttazzo D, Kannike K et al. Phys. Rev. D, 2013, **87**: 115018
26 Paul de Jong for ATLAS and CMS collaboration. Proceed-
ings of Physics in Collision 2012, ATL-PHYS-PROC-**2012-244**, arXiv: hep-ex/1211.3887
27 CMS collaboration. CMS-SUS-**13-011**, CMS-SUS-**13-003**, PAS-SUS-**13-017**
28 ATLAS collaboration. ATLAS-CONF-**2013-093**, ATLAS-CONF-**2013-062**, ATLAS-CONF-**2013-089**
29 Planck collaboration. arXiv: astro-ph.CO/1303.5076
30 Stockinger D. J. Phys. G, 2007, **34**: 45
31 http://www.th.u-psud.fr/NMHDECAY/nmssmtools.html
32 Bechtle P et al. Comput. Phys. Commun., 2010, **181**: 138-167; Bechtle P et al. Comput. Phys. Commun., 2011, **182**: 2605–2631; Bechtle P et al. PoS CHARGED., 2012, **2012**: 024; Bechtle P et al. BONN-TH-**2013-21**, DESY **13-110**, arXiv: hep-ph/1311.0055
33 Bechtle P, Heinemeyer S. BONN-TH-**2013-07**, DESY **13-078**, arXiv: hep-ph/1305.1933; Stal O, Stefaniak T. BONN-TH-**2013-20**, arXiv: hep-ph/1310.4039
34 Bélanger G, Dumont B, Ellwanger U et al. Phys. Rev. D, 2013, **88**: 075008
35 Allanach B et al. Comput. Phys. Commun., 2009, **180**: 8
36 Djouadi A. Phys. Rept., 2008, **459**: 1
37 Buras A J, Chankowski P H, Rosiek J, Slawianowska L. Nucl. Phys. B, 2003, **659**: 3
38 Misiak M et al. Phys. Rev. Lett., 2007, **98**: 022002
39 Hiller G. Phys. Rev. D, 2004, **70**: 034018
40 Domingo F, Ellwanger U. J. High Energy Phys., 2007, **0712**: 090
41 Elliott T, King S F, White P L. Phys. Rev. D, 1994, **49**: 2435-2456
42 Spergel D N, Bean R. Astrophys. J. Suppl., 2007, **170**: 377
43 LHC Higgs Cross Section Working Group. https://twiki.cern. ch/twiki/bin/view/LHCPhysics/CrossSections
44 CMS collaboration. CMS-HIG-**13-001**, https://twiki.cern.ch/ twiki/bin/view/CMSPublic/PhysicsResultsHIG
45 ATLAS collaboration. ATLAS-CONF-**2013-007**, https://twiki. cern.ch/twiki/bin/view/AtlasPublic/HiggsPublicResults
46 CMS collaboration. CMS-HIG-**13-016**, https://twiki.cern.ch/ twiki/bin/view/CMSPublic/PhysicsResultsHIG